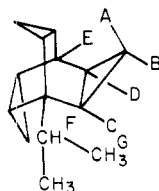


Table IV.  $^1\text{H}$  NMR Chemical Shifts ( $\delta$ , ppm relative to Me<sub>4</sub>Si) and Coupling Constants (Hz) of 1-Isopropyltrishomobarrelene



chemical shifts ( $\pm 0.001$  ppm)

$\delta_A$	$\delta_B$	$\delta_C$	$\delta_D$	$\delta_E$	$\delta_F$	$\delta_G$
0.767	0.041	0.364	0.497	2.366	1.697	0.992

coupling constants ( $\pm 0.3$  Hz)

$J_{AB}$	$J_{AD}$	$J_{AC}$	$J_{BD}$	$J_{BC}$	$J_{CD}$	$J_{DE}$	$J_{FG}$
(-) 5.3	3.8	3.8	7.8	7.8	8.1	4.7	6.8

than 0.1 ppm. The concentrations for the measurements of the substituted trishomobarrelenes 10a-d are given in Table III.

For the assignment of the carbon resonances the following criteria were employed: 6, off-resonance decoupling<sup>19</sup> and  $^1J(^{13}\text{C}$ ,

$^1\text{H}$ ) values of 134.5 and 127.0 Hz for the CH and CH<sub>2</sub> groups, respectively; 7, C-9 triplet at highest field ( $^1J = 163$  Hz), C-2,3 doublet ( $^1J = 165$  Hz), C-1,4 doublet ( $^1J = 134$  Hz), C-5,6 and C-7,8 triplets; 8, C-9 and C-9a triplets ( $^1J = 159$  Hz) at highest field, C-2,3 and C-5,6 doublets ( $^1J = 161, 166$  Hz), C-1,4 doublet ( $^1J = 136.2$  Hz), C-7,8 triplet ( $^1J = 128.7$  Hz); 9, C-9 triplet ( $^1J = 158$  Hz), C-2,3,5,6 doublet ( $^1J = 164$  Hz), C-7,8 triplet ( $^1J = 128$  Hz), C-1,4 doublet ( $^1J = 133$  Hz); 10, off-resonance decoupling and relative intensity; 18, C-7,8 triplet ( $^1J = 126$  Hz), C-2,3,5,6 doublet of highest relative intensity ( $^1J = 166$  Hz), C-1,4 doublet ( $^1J = 137$  Hz), C-9,9a doublet ( $^1J = 171$  Hz).

**Acknowledgment.** We are indebted to the Deutsche Forschungsgemeinschaft and the Fonds der Chemischen Industrie for generous support.

**Registry No.** 6, 280-33-1; 7, 278-80-8; 8, 63180-69-8; 9, 63180-71-2; 10, 70469-89-5; 10a, 74925-50-1; 10b, 74925-51-2; 10c, 74925-52-3; 10d, 74925-53-4; 18, 28339-41-5.

(19) H. Günther, "NMR Spectroscopy", J. Wiley & Sons, New York, 1980, p 310 ff.

## Hydrolysis Kinetics of an Amphiphilic Fatty Acid Ester. Real and Artfactual Effects of Reactant-Product Aggregation

Alim A. Fatah and Leslie M. Loew\*

Department of Chemistry, State University of New York at Binghamton, Binghamton, New York 13901

Received April 28, 1980

The hydrolysis of (4-(palmitoyloxy)phenyl)trimethylammonium iodide in 30% aqueous ethanol is accompanied by a sudden increase in solution turbidity if the initial ester concentration is  $>10^{-4}$  M. The turbidity is attributed to aggregates of the palmitic acid product containing a small proportion of the ester. A methodology for extracting the reaction rate from the absorbance change requires the combination of a dual-wavelength photometer and a direct fit of the data to a single exponential. It is found that the reaction rate is left largely unaffected by the aggregation process. Turbidity measurements and microscopic examination reveal particle sizes in the 1-2- $\mu\text{m}$  range where the wavelength dependence of light scattering is weaker than that for smaller particles. This improves the effectiveness of the dual-wavelength technique which uses the absorbance at a reference wavelength to cancel out drift due to variations in either source intensity or sample turbidity. Thus, artifacts due to turbidity changes, even in these strongly scattering preparations, are eliminated.

### Introduction

The study of reactions in micellar systems is an extremely active and maturing area of physical organic chemical research.<sup>1</sup> It owes its rapid development, in part, to the fascination and importance of chemistry at an interface and, in part, to the applicability of the well-established techniques and analyses of solution kinetics.

As more complex systems are studied, including better models for biological membranes, these traditional techniques may have to be modified. Biochemists and biophysicists have long had to contend with turbid preparations where the change in absorbance due to an intracellular reaction of interest is small compared to a relatively constant scattering and absorbing background. Chance developed the dual-wavelength photometer to deal with these situations.<sup>2</sup> The particle size would have to be quite large ( $>300$  Å) for scattering to interfere with the large

absorbance changes which can be conveniently chosen in a homogeneous or micellar reaction. We report here a simple saponification of a surfactant ester which is complicated by formation of large aggregates of reactant and product and an accompanying sudden drastic increase in turbidity unlike anything normally encountered with either biological or chemical reactions. The dual-wavelength technique of Chance is simplified to allow the separation of the real from the artifactual effects of the aggregation on the reaction kinetics.

### Experimental Section

**Materials.** By the procedure of Bruce et al.<sup>3</sup> for the dodecanoic acid ester, (4-(palmitoyloxy)phenyl)trimethylammonium iodide was prepared by trifluoroacetic anhydride induced condensation of palmitic acid and (4-hydroxyphenyl)trimethylammonium iodide. Recrystallization first from ethanol-water and then from methanol-diethyl ether gave analytically pure ester in 54% yield: mp 156-158 °C; IR (Nujol mull) 1760  $\text{cm}^{-1}$ ; NMR ( $\text{Me}_2\text{SO}-d_6$ )  $\delta$  0.82 (t,  $J = 7$  Hz, 3 H), 1.1-2.0 (br s, 28 H), 3.63

(1) Fendler, J. H.; Fendler, E. J. "Catalysis in Micellar and Macromolecular Systems"; Academic Press: New York, 1975. Cordes, E. H. "Reaction Kinetics in Micelles"; Plenum: New York, 1973.

(2) Chance, B.; Graham, N.; Sorge, J.; Legallain, V. *Rev. Sci. Inst.* 1972, 43, 62 and references cited therein.

(3) Bruce, T. C.; Katzhendler, J.; Fedor, L. R. *J. Am. Chem. Soc.* 1968, 90, 1333.

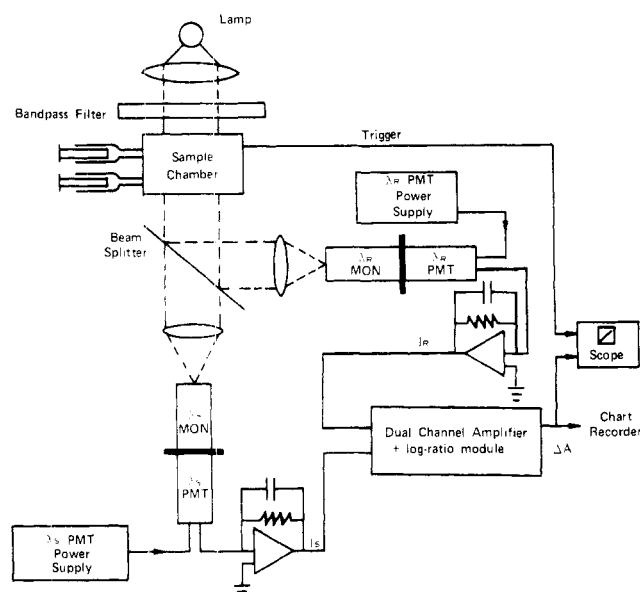


Figure 1. Block diagram of the dual-wavelength photometer.

(s, 9 H), 7–8 (AA'–BB', 4 H). Anal. Calcd for  $C_{25}H_{44}INO_2$ : C, 58.04; H, 8.51; I, 24.55; N, 2.71. Found: C, 57.94; H, 8.77; I, 24.43; N, 2.66. (Analysis was performed by Atlantic Microlab, Inc., Atlanta, GA.)

Solutions for kinetic measurements were made of 70% pH 9 aqueous buffer (0.1 M  $H_3BO_3$ –KCl–NaOH, Fisher Scientific Co.) and 30% ethanol (v/v). The final pH of this solution was 9.8. Solutions for turbidity measurements were made of 70% pH 7 aqueous buffer (0.05 M  $KH_2PO_4$ –NaOH, Fisher Scientific Co.) and 30% ethanol (v/v). These solutions were made up immediately prior to an experiment, using an ethanolic stock solution of the ester substrate and/or palmitic acid as appropriate. All solvents were deaerated by boiling and cooling under  $N_2$ . Double glass distilled water was used where necessary.

**Apparatus.** Turbidity measurements and some of the kinetic plots were carried out with a Beckman Model 25 spectrophotometer. Water circulation through the cuvette holder from a Lauda K2R thermostatted bath maintained the temperature of the cuvette at  $35.0 \pm 0.1$  °C. For the kinetic runs, the appearance of the phenolate was monitored at 289 nm. Turbidity measurements are reported in absorbance units and were taken at several wavelengths as outlined under Results.

The kinetic course of reactions which were complicated by concurrent changes in turbidity was followed with a dual-wavelength photometer constructed in this laboratory. The optical system is outlined in Figure 1. The sample chamber consists of a conventional cuvette holder in a thermostated aluminum block over an air-driven magnetic stirrer; this can be replaced with an Aminco-Morrow stopped-flow mixing device for faster reactions. The collimated beam from a 75-W xenon arc lamp (Oriel Corporation) is passed through the sample after passing through a Corning 7-54 UV-transmitting black glass filter, a water filter, and, if necessary, a neutral density filter. After emerging from the sample the light is divided with a 50% beam splitter and focused onto the 2-mm slits of a pair of monochromators (Instruments SA, Inc., Model H2O-UV). The output of the two photomultipliers (EM1-Gencom, Inc., 9781R) is sent into the two channels of a simple amplifier which takes the base 10 logarithm of their ratio; if the initial intensities are balanced electronically on a blank sample by adjusting the high voltages across the two photomultiplier dynode chains, this ratio is equivalent to the difference in absorbance between the two wavelengths at which the monochromators are set. The amplifier is built around an Analog Devices, Inc., 757 N log-ratio module. The amplifier has outputs for the transmission at each wavelength in addition to the difference in absorbance ( $\Delta A$ ). Both  $\Delta A$  and the transmittance at the reference wavelength are presented to a 2-pen recorder during a typical kinetic run.

A Leitz Ortholux II microscope was used to examine and size the aggregated particles. An achromatic 100 power oil immersion

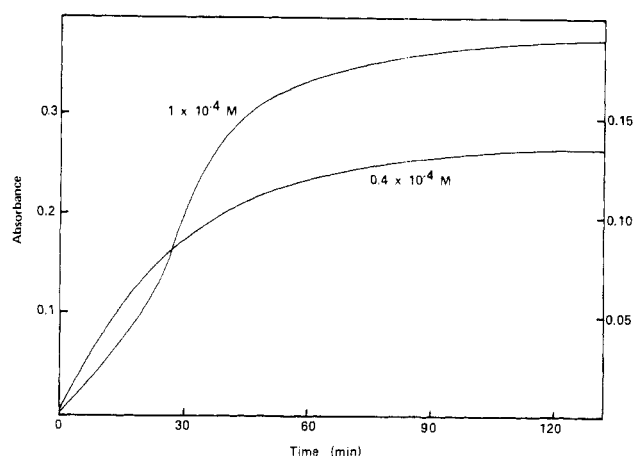


Figure 2. Absorbance change with time for saponification of the ester at two initial concentrations using a standard double-beam spectrophotometer. The left ordinate applies to  $10^{-4}$  M, the right to  $4 \times 10^{-5}$  M.

Table I. Experimental Rate Constants for Ester Hydrolysis Measured under Various Conditions

ester concentration, M	rate constant [standard deviation] $\times 10^2$ , $\text{min}^{-1}$		
	double beam	dual $\lambda$ (289–314 nm)	dual $\lambda$ (298–303 nm)
$2 \times 10^{-5}$	3.11 [0.23]	3.17 [0.21]	<i>b</i>
$4 \times 10^{-5}$	3.08 [0.30]	3.31 [0.15]	<i>b</i>
$1 \times 10^{-4}$	<i>a</i>	2.91 [0.17]	3.41 [0.05]
$1.4 \times 10^{-4}$	<i>a</i>	2.71 [0.12]	3.19 [0.16]
$2 \times 10^{-4}$	<i>a</i>	2.12 [0.28]	3.35 [0.06]

<sup>a</sup> The absorbance vs. time plots do not fit a single exponential. <sup>b</sup> The  $\Delta A$  change is too small to provide a reproducible rate constant with the dual wavelength apparatus described here.

objective proved necessary. The eyepiece micrometer was calibrated with a 2 mm/200 division stage micrometer.

**Kinetics.** Conventional first-order kinetic treatments of the data were possible with either the double-beam or dual-wavelength apparatus up to  $10^{-4}$  M (see Discussion). At [ester]  $> 10^{-4}$  M the dual-wavelength photometer had to be used. The rate constants were obtained from a variational fit of  $\Delta A$  to a single exponential with the APL program KINETICS. Data for each run were taken to at least 4 half-lives and the rate constants presented are means of at least 4 runs. Plots of  $\log [Abs(t) - Abs(\infty)]$  vs. time are presented in the text for purposes of discussion and usually provided rate constants within the standard deviation of the computer fits if turbidity did not develop.

## Results and Discussion

The kinetic traces obtained with a conventional double-beam spectrophotometer for the saponification of (4-(palmitoyloxy)phenyl)trimethylammonium iodide (hereafter, "the ester") at two different concentrations are displayed in Figure 2. At  $4 \times 10^{-5}$  M, a pseudo-first-order rate constant is obtained from the simple exponential appearance of the phenolate absorbance; this rate constant is reproducible up to ester concentrations of  $\sim 10^{-4}$  M (Table I). At concentrations above this point, the behavior illustrated in Figure 2 develops and makes analysis of the kinetics impossible. The break in the exponential absorbance increase is attributable to a sudden increase in the turbidity of the sample solution. The solution remains clear if a surfactant is added (20 mM hexadecyltrimethylammonium bromide) or if the percentage of ethanol is increased, implying that the turbidity is caused by large aggregates; the rate of the reaction is, of course, also perturbed by these additives.

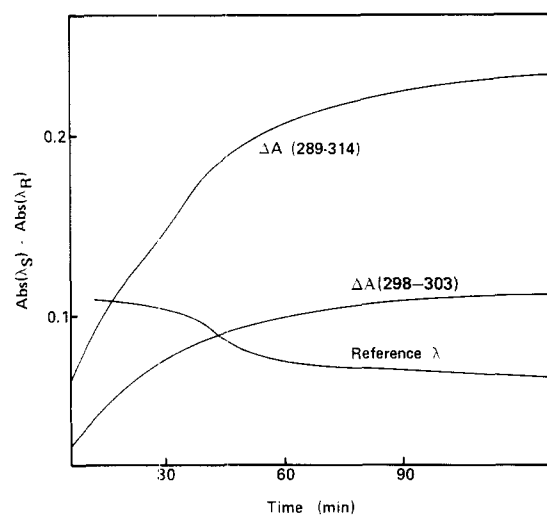


**Figure 3.** Kinetic course of the saponification of the  $10^{-4}$  M ester monitored with the dual-wavelength photometer. The curve labeled with  $\Delta A$  (289-314) was obtained with reference and sample wavelengths of 314 and 289 nm, respectively; the curve labeled  $\Delta A$  (303-298) was obtained with 303 and 298 nm, respectively. Also shown is the variation in transmitted intensity at 314 nm (intensity scale not shown).

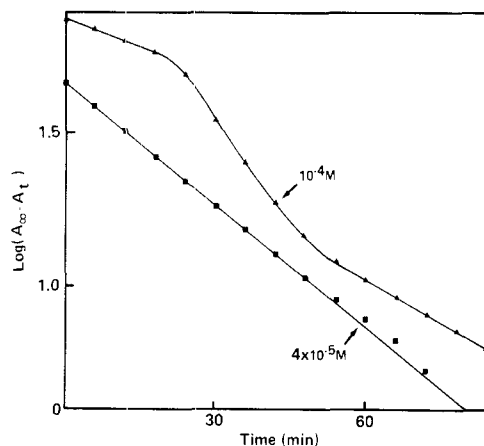


**Figure 4.** Pseudo-first-order kinetic plots of the data displayed in Figure 2.

The dual-wavelength photometer eliminates the distortion due to the sudden appearance of turbidity as illustrated in Figure 3. Typical kinetic plots corresponding to the traces in Figures 2 and 3 are displayed in Figures 4 and 5 and the data are summarized in Table I. Below  $10^{-4}$  M the rate is independent of [ester] and can be equally well determined with either the double-beam or the dual-wavelength photometer. Above  $10^{-4}$  M only the dual-wavelength photometer gives undistorted kinetic plots, yielding pseudo-first-order rate constants essentially identical with those of  $<10^{-4}$  M experiments. The two wavelengths which provide the best data are 298 and 303 nm; both of these are on the steeply descending red side of the phenolate absorption band. If the 289-314-nm wavelength pair is used, a much larger change in  $\Delta A$  is obtained, but a small inflection at the onset of the turbidity is visible in the kinetic trace (Figure 3). This leads to a distortion in the first-order kinetic plot for this wavelength pair (Figure 5) and somewhat less reproducible rate constants (Table I). The rate constants extracted from this distorted data show a small artifactual decrease in rate with increasing [ester].

The rationale behind this application of the dual-wavelength technique is that by subtracting the absorbance at one wavelength, at which the absorbance of the kinet-

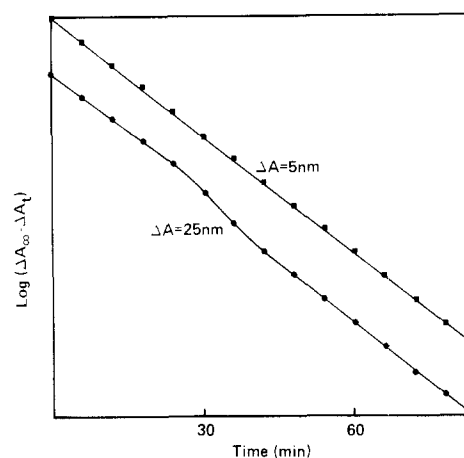


**Figure 5.** Pseudo-first-order kinetic plots of the data displayed in Figure 3.

ically active chromophore is small, from the absorbance at a wavelength in the chromophore absorption band, the distortions due to turbidity changes can be largely cancelled. Thus, a single solution serves as both sample and reference. The success of this approach depends, of course, on the near identity of the turbidity components of the observed absorbances at the two chosen wavelengths. At the concentrations of ester being used in the present work, the large turbidities that are observed can arise only from particles much larger than the wavelength. Therefore, the familiar  $\lambda^{-4}$  dependence of the turbidity does not apply, a much gentler wavelength dependence having been found both experimentally and theoretically for monodisperse suspensions of large particles.<sup>4,5</sup> The polydispersity of our suspended particles would be expected to dampen any wavelength dependence still further. The apparent absorbances at 400, 314, and 289 nm were recorded after 6 half-lives as 0.19, 0.30, and 0.73 A, respectively, for a sample initially  $2 \times 10^{-4}$  M in ester to quantify these assumptions. If these figures are corrected for the absorbance due to the phenolate at these respective wavelengths, the turbidity contributions are determined as 0.19, 0.28, and 0.30 A. Thus, by taking the difference in absorbance between 289 and 314 nm, all but 7% of the turbidity change is being cancelled out; this residual turbidity contribution, in turn, amounts to only 2% of the total absorbance change resulting from production of phenolate. On the other hand, a greater wavelength sensitivity would be expected at least at the initial appearance of turbidity when average particle size is presumably still small. This is indeed manifested by the slight inflection seen in all the dual  $\lambda$  traces at the onset of turbidity (Figures 3 and 5) when  $\Delta\lambda = 25$  nm and the resultant distorted rate constants already noted. Thus, only with  $\Delta\lambda = 5$  nm can reliable data be obtained throughout.

The aggregation process has its own peculiar kinetic behavior which can be investigated at pH 7.6, independent of the absorbance change due to the reaction. A solution of  $1.5 \times 10^{-4}$  M palmitic acid and  $5 \times 10^{-5}$  M ester in 30% ethanol-70% aqueous buffer (0.05 M  $\text{KH}_2\text{PO}_4$ -NaOH) is initially clear; turbidity develops within 10 min. This behavior is completely reproducible and is analyzed in Figure 6. The turbidity changes are qualitatively and quantitatively different at the three chosen wavelengths. This is completely consistent with the Mie theory applied to scattering of large particles.<sup>5,6</sup> By use of this theory

(4) Hodkinson, J. R. In "Electromagnetic Scattering"; Kerker, M., Ed.; Pergamon Press: New York, 1963; pp 87-100.

(5) Heller, W., ref 4, pp 101-122.

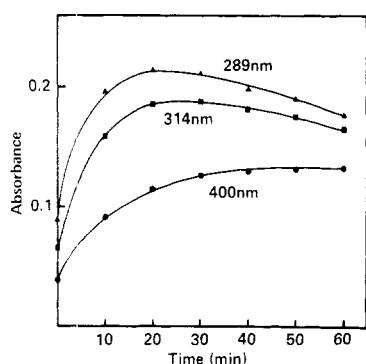


**Figure 6.** Development of turbidity in a solution of  $5 \times 10^{-5}$  M ester and  $1.5 \times 10^{-4}$  M palmitic acid in 30% aqueous ethanol, pH 7.6.

qualitatively, Figure 6 can be interpreted in terms of the growth of the suspended particles. Above a critical diameter, the scattering begins to *fall* with increasing particle size, finally leveling off to the classical scattering limit; assuming a refractive index of 1.45 for monodisperse spherical scattering particles, the critical diameter is ca.  $4 \lambda$  (see, in particular, Figure 3 in ref 5). In Figure 6, maxima are reached at 23, 30, and 50 min for turbidity monitored at 289, 314, 400 nm, respectively; broadly applying the factor of  $4 \lambda$  one obtains a picture of an initially fast increase in particle diameter to ca.  $1 \mu\text{m}$  which gradually slows and levels off.

Microscopic examination of the reaction mixture initially  $1.4 \times 10^{-4}$  M in ester revealed particles of remarkable uniformity, averaging approximately  $1.5 \mu\text{m}$  in diameter, after 4 h of reaction ( $\sim 10$  half-lives). Examination of the solution used to generate Figure 6 24 h after its preparation revealed less homogeneous particles ranging up to  $\sim 15 \mu\text{m}$ .

Interestingly, neither the ester nor the palmitic acid by themselves gives rise to turbidity in the relevant concentration range. The turbidity at the end of the reaction must be due, therefore, to metastable aggregates of palmitic acid with perhaps a very small proportion of entrapped residual ester. Indeed, the turbidity of the reac-

tion mixture fades gradually with a half-life of approximately 3.5 days. Also, an experiment with the concentrations of ester and palmitic acid at  $1.5 \times 10^{-4}$  M and  $5 \times 10^{-5}$  M, respectively (i.e., reversal of the concentrations used to generate Figure 6), revealed a marginally small increase in turbidity at  $35^\circ\text{C}$ .

This picture of the aggregate composition is consistent with the insensitivity of the hydrolysis rate to the aggregation. It should be emphasized that this insensitivity is revealed only if the 298–303-nm wavelength pair is used (as has been already discussed) and only if the absorption change is fit directly to an exponential. Distortions in the single exponential fit are apparent if the data beyond ca. 5 half-lives is included; at this stage in the reaction a significant portion of the residual ester is surely associated with the palmitic acid aggregates, effecting a rate retardation. Of course, below  $1 \times 10^{-4}$  M ester, any method of data analysis, including a conventional log plot, provides rate constants identical with those obtained with the exponential fit of the dual-wavelength data.

### Conclusion

The turbidity problem associated with this reaction is quite severe. Both a dual-wavelength apparatus and a variational fit of the exponential increase in absorbance were required to substantiate that the aggregation process does not affect the reaction until almost all the reactant has been consumed. Even when upwards of 90% of the turbidity change is cancelled from data, artifactual changes in the derived kinetics cannot be avoided. It is appropriate to advocate that adoption of this general methodology be strongly considered for experiments involving kinetics in micelles or vesicles where changes in the concentration of reactant and product can often lead to substantial variations in the degree of aggregation of surfactant or lipid.

**Acknowledgment.** We thank Mr. David Smart for providing us with the KINETICS program. This work was supported by the Research Corporation and by Grant Number CA-23838 awarded by the National Cancer Institute, USPHS.

**Registry No.** (4-(Palmitoyloxy)phenyl)trimethylammonium iodide, 74835-35-1.

(6) Sinclair, D. *J. Opt. Soc. Am.* 1947, 37, 475.